

# **$Z_2$ -Regge versus Standard Regge Calculus in two dimensions**

E. Bittner, A. Hauke, H. Markum, J. Riedler

*Institut für Kernphysik, Technische Universität Wien, A-1040 Vienna, Austria*

C. Holm

*Max-Planck-Institut für Polymerforschung, D-55128 Mainz, Germany*

W. Janke

*Institut für Physik, Johannes Gutenberg-Universität Mainz, D-55099 Mainz, Germany*

*Institut für Theoretische Physik, Universität Leipzig, D-04109 Leipzig, Germany*

(April 30, 2018)

## Abstract

We consider two versions of quantum Regge calculus. The Standard Regge Calculus where the quadratic link lengths of the simplicial manifold vary continuously and the  $Z_2$ -Regge Model where they are restricted to two possible values. The goal is to determine whether the computationally more easily accessible  $Z_2$  model still retains the universal characteristics of standard Regge theory in two dimensions. In order to compare observables such as average curvature or Liouville field susceptibility, we use in both models the same functional integration measure, which is chosen to render the  $Z_2$ -Regge Model particularly simple. Expectation values are computed numerically and agree qualitatively for positive bare couplings. The phase transition within the  $Z_2$ -Regge Model is analyzed by mean-field theory.

PACS: 04.60.Nc

Typeset using REVTeX

## I. INTRODUCTION

Standard Regge Calculus (SRC) [1] provides an interesting method to explore quantum gravity in a non-perturbative fashion [2]. The infinite degrees of freedom of Riemannian manifolds are reduced by discretization, that is, SRC deals with piecewise linear spaces described by a finite number of parameters. A manifold is approximated by a simplicial lattice with *fixed* coordination numbers, as opposed to the dynamical triangulated random surface (DTRS) method [3] where the coordination numbers are treated as the dynamical degrees of freedom. This leaves in SRC the quadratic link lengths  $q$  as gravitational degrees of freedom which are constraint by triangle inequalities. Since analytical treatments have proven to be difficult, this approach has been extensively studied through numerical computer simulations during the last ten years [4,5]. Although the computer codes can be efficiently vectorized, large scale simulations are still a very time demanding enterprise. One therefore seeks for suitable approximations which will simplify the SRC and yet retain most of its universal features.

The  $Z_2$ -Regge Model ( $Z_2$ RM) [6] could be such a desired simplification. Here the quadratic link lengths  $q$  of the simplicial complexes are restricted to take on only the two values  $q_l = 1 + \epsilon\sigma_l, 0 < \epsilon < \epsilon_{max}, \sigma_l = \pm 1$ , in close analogy to the ancestor of all lattice models, the Lenz-Ising model. To test whether this simpler model is in a reasonable sense still similar to SRC, i.e. shares the same universal properties, we study both models in two dimensions and compare a number of observables for one particular lattice size. Moreover we estimate in both models the critical exponent  $\eta_\phi$  of the Liouville field susceptibility by performing a finite-size scaling analysis on moderately sized lattices.

Although some models for 2d-quantum gravity have been exactly solved via the matrix model approach [7] and with the help of conformal field theory [8], the relation of those approaches to SRC is not yet understood. There are even severe discrepancies between the alternative discrete approach, the DTRS method [3], and SRC. Especially the functional integration measure in SRC is under heavy debate [9]. In an effort to clarify the role of the

measure the conventional definition of diffeomorphisms has been employed, assuming that a piecewise linear space, i.e. a Regge surface, is *exactly* invariant under the action of the full diffeomorphism group [10]. After a conformal gauge fixing was performed in the continuum formalism, it was shown that the evaluation of the non-local Faddeev-Popov determinant by using such a Regge regularization leads to the usual Liouville field theory results in the continuum limit. All that is based on a description of piecewise linear manifolds with deficit angles, not edge lengths, and is mostly taken as an argument that the correct measure of Standard Regge Calculus has to be non-local. However, to our knowledge it is not obvious that this argument carries over to a discretized Lagrangian, which is formulated in terms of fluctuating edge lengths, obeying triangle equalities, and which is *not* invariant under the diffeomorphism group due to the presence of curvature defects: different assignments of edge lengths correspond to different physical geometries, and as a consequence there are no gauge degrees of freedom in Standard Regge Calculus, apart from special geometries (like flat space) [11]. Therefore we do not include a gauge fixing term and rely in this work still on a local measure. Our main goal in this present investigation is not to resolve the measure question but to explore the phase behavior of the  $Z_2$ RM and its relation to SRC. We will show that the discretized  $Z_2$ RM does not suffer from unphysical gauge degrees of freedom. If both SRC and  $Z_2$ RM for certain local measures lie in the same universality class one can hope to learn about physical observables using this simplified approach.

The rest of the paper is organized as follows: In Chapter II we briefly review the Standard Regge Model as well as the  $Z_2$ -Regge Model. In Chapter III we introduce the observables and discuss important scaling relations. The details of the Monte Carlo simulations and the results are presented in Chapter IV. Chapter V deals with a mean-field approach for the  $Z_2$ RM to discuss the observed phase transition in that specific model. Finally Chapter VI ends with our conclusion.

## II. MODELS

Starting point for both Standard Regge Calculus and the  $Z_2$ -Regge Model is Regge's discrete description of General Relativity in which space-time is represented by a piecewise flat, simplicial manifold: the Regge skeleton [1,4]. The beauty of this procedure is that it works for any space-time dimension  $d$  and for metrics of arbitrary signature. The Einstein-Hilbert action translates into

$$I(q) = \lambda \sum_{s^d} V(s^d) - 2\beta \sum_{s^{d-2}} \delta(s^{d-2}) V(s^{d-2}) , \quad (2.1)$$

with the quadratic edge lengths  $q$  describing the dynamics of the lattice,  $\lambda$  being the cosmological constant, and  $\beta$  the bare Planck mass squared. The first sum runs over all  $d$ -simplices  $s^d$  of the simplicial complex and  $V(s^d)$  is the  $d$ -volume of the indicated simplex. The second term represents the curvature of the lattice, that is concentrated on the  $(d-2)$ -simplices leading to deficit angles  $\delta(s^{d-2})$ , and is proportional to the integral over the curvature scalar in the classical Einstein-Hilbert action of the continuum theory. The connectivity of the edges, in simplicial terminology called the incidence matrix, is fixed from the beginning through the simplicial decomposition of the manifold under consideration. Any smooth manifold can be approximated by a Regge skeleton with arbitrarily small deficits simply by using a sufficient number of links and arranging them appropriately.

### A. Standard Regge Calculus

In two dimensions Regge's discretization procedure is easily illustrated by choosing a triangulation of the considered surface. Each triangle then represents a part of a piecewise linear manifold. The net of triangles itself is a two-geometry, with singular (non-differentiable) points located at the vertices of the net. In the presence of curvature a vector that is parallel transported around a vertex experiences a rotation by the deficit angle  $\delta_i = 2\pi - \sum_{t \supset i} \theta_i(t)$ , where  $\theta_i(t)$  are the dihedral angles of the triangles  $t$  attached to vertex  $i$ . The integral of the

scalar curvature over the simplicial complex  $K$  in two dimensions is a topological invariant due to the Gauss-Bonnet theorem. Its simplicial analogue reads as

$$\sum_{i \supset K} \delta_i = 2\pi\chi(\mathcal{M}) , \quad (2.2)$$

where  $\chi = 2(1 - g)$  is the Euler characteristic of the manifold  $\mathcal{M}$  expressed by the number of handles  $g$  in  $\mathcal{M}$ .

In the exceptional case of flat skeletons one can move a vertex on the surface, keeping all the neighbors fixed, without violating the triangle inequalities, such that different configurations triangulate the same (flat) geometry. This transformation has two parameters and is an exact invariance of the action, but does not exist in general. When space is curved the invariance is only an approximate one. In the limit of increasing number of links local gauge invariance, that is the continuum diffeomorphism group should be recovered.

A quantization of the above action (2.1) proceeds by evaluating the path integral

$$Z = \int D[q] e^{-I(q)} . \quad (2.3)$$

In principle the functional integration should extend over all metrics on all possible topologies, but, as is usually done, we restrict ourselves to one specific topology, the torus,  $\mathcal{M} = T^2$ . Consequently the Euler characteristic  $\chi(T^2)$  vanishes in (2.2) and the action (2.1) consists only of a cosmological constant  $\lambda$  times the sum over all triangle areas  $A_t$ . The path-integral approach suffers from a non-uniqueness of the integration measure, even the need for a non-local measure is advocated. However, some of the proposed non-local measures do not agree with their continuum counterparts in the weak field limit, which is a necessary condition for an acceptable discrete measure [9]. This property however is fulfilled for the standard simplicial measure [12]

$$\int D[q] = \Pi_l \int \frac{dq_l}{q_l^m} \mathcal{F}_\eta(q_l) , \quad (2.4)$$

with  $m \in \mathbb{R}$  permitting to investigate a 1-parameter family of measures. The function  $\mathcal{F}_\eta(q_l)$  constrains the integration to those Euclidean configurations of link lengths which

do not violate the triangle inequalities. The positive parameter  $\eta$  modifies the triangle inequalities to  $l_3 \leq (l_1 + l_2)(1 - \eta)$  and  $l_3 \geq |l_1 - l_2|(1 + \eta)$ , so that very thin triangles are suppressed. This is not necessary on theoretical grounds, but will be useful for the Monte Carlo evaluation of the path integral.

Hence the model considered here is characterized by the partition function

$$Z = \left[ \prod_l^{N_1} \int_0^\infty dq_l q_l^{-m} \right] \mathcal{F}_\eta(\{q_l\}) e^{-\lambda \sum_i A_i} , \quad (2.5)$$

where  $N_1$  is the number of links and  $A_i = \sum_{t \supset i} A_t / 3$  denotes the barycentric area with  $A_t$  being the area of a triangle  $t$ . A specific choice of the value of the parameter  $m$  will be discussed in the next section.

As discussed above, the numerical computations of (2.5) (for technical details see Chapter IV) do not run into the diffeomorphism problem by summing over distinct simplicial lattices without fixing a gauge. Still the question arises whether one double-counts some classes of geometries in this way, e.g., one may argue from the above that flat geometries are over-represented, though simulations give no hints on that.

## B. $Z_2$ -Regge Model

In the  $Z_2$ -Regge Model [6] the squared edge lengths  $q_l$  are allowed to take on only the two values

$$q_l = 1 + \epsilon \sigma_l , \quad 0 \leq \epsilon < \epsilon_{max} , \quad \sigma_l = \pm 1 , \quad (2.6)$$

where the parameter  $\epsilon$  is chosen such that the Euclidean triangle inequalities are fulfilled for all  $q_l$ 's, i.e.  $\mathcal{F}_\eta = 1$  for all configurations  $\{q_l\}$ . There exist  $2^{N_1}$  different configurations and for finite  $\epsilon$  and link lengths none of them can be transformed smoothly into each other. A further nice attribute of the  $Z_2$ RM is its accordance with lattice perturbation theory. As described in [13], (2.6) can be viewed as weak-field expansion around flat space, implicitly having performed a conformal gauge fixing. On each triangle the metric tensor assumes

the form  $g_{\mu\nu}(\Delta) = (1 + \epsilon)\delta_{\mu\nu}$ . However a finite  $\epsilon$  inhibits local conformal transformations. Since triangles share links, rescaling lengths on one particular triangle would necessitate the same rescaling for the neighboring triangle and so on. What remains only is a global transformation. In the continuum limit the local conformal degree of freedom should be restored.

Using (2.6) the measure (2.4) can be replaced by

$$\sum_{\sigma_l=\pm 1} \exp[-m \sum_l \ln(1 + \epsilon \sigma_l)] = \sum_{\sigma_l=\pm 1} \exp[-N_1 m_0(\epsilon) - \sum_l m_1(\epsilon) \sigma_l] , \quad (2.7)$$

where  $m_0 = -\frac{1}{2}m\epsilon^2 + O(\epsilon^4)$  and  $m_1 = m[\epsilon + \frac{1}{3}\epsilon^3 + O(\epsilon^5)] = mM$  with

$$M = \sum_{i=1}^{\infty} \frac{\epsilon^{2i-1}}{2i-1} = \frac{1}{2} \ln \frac{1+\epsilon}{1-\epsilon} . \quad (2.8)$$

The area of a single triangle  $t$  with squared edge lengths  $q_1, q_2, q_l$  can be expressed as

$$\begin{aligned} A_t &= \frac{1}{2} \left| \begin{array}{cc} q_1 & \frac{1}{2}(q_1 + q_2 - q_l) \\ \frac{1}{2}(q_1 + q_2 - q_l) & q_2 \end{array} \right|^{\frac{1}{2}} = \\ &= \frac{1}{2} \left\{ \frac{3}{4} + \frac{1}{2}(\sigma_1 + \sigma_2 + \sigma_l)\epsilon + \frac{1}{2}(\sigma_1\sigma_2 + \sigma_1\sigma_l + \sigma_2\sigma_l - \frac{3}{2})\epsilon^2 \right\}^{\frac{1}{2}} . \end{aligned} \quad (2.9)$$

Expanding  $A_t$  the series consists only of terms up to  $\sigma^3$  since  $\sigma_i^2 = 1$ . Therefore  $A_t$  can be written as

$$A_t = c_0(\epsilon) + c_1(\epsilon)(\sigma_1 + \sigma_2 + \sigma_l) + c_2(\epsilon)(\sigma_1\sigma_2 + \sigma_1\sigma_l + \sigma_2\sigma_l) + c_3(\epsilon)\sigma_1\sigma_2\sigma_l . \quad (2.10)$$

Computing the four possible values for the triangle areas and comparing with (2.10) results in exact solutions for the coefficients  $c_i$ ,

$$\begin{aligned} c_0 &= \frac{1}{32} \left[ 2\sqrt{3} + 3\sqrt{(1-\epsilon)(3+5\epsilon)} + 3\sqrt{(1+\epsilon)(3-5\epsilon)} \right] , \\ c_1 &= \frac{1}{32} \left[ 2\sqrt{3}\epsilon + \sqrt{(1-\epsilon)(3+5\epsilon)} - \sqrt{(1+\epsilon)(3-5\epsilon)} \right] , \\ c_2 &= \frac{1}{32} \left[ 2\sqrt{3} - \sqrt{(1-\epsilon)(3+5\epsilon)} - \sqrt{(1+\epsilon)(3-5\epsilon)} \right] , \\ c_3 &= \frac{1}{32} \left[ 2\sqrt{3}\epsilon - 3\sqrt{(1-\epsilon)(3+5\epsilon)} + 3\sqrt{(1+\epsilon)(3-5\epsilon)} \right] . \end{aligned} \quad (2.11)$$

Obviously one must have  $\epsilon < \frac{3}{5} = \epsilon_{max}$  for the triangle areas to be real and positive. In the simulations described below we used  $\epsilon = 0.5$  but the special choice of  $\epsilon$  does not affect our numerical results except for the value of the critical coupling ( $\lambda_c$ ) as one can infer from the next equation. It is obtained by inserting (2.7) and (2.10) into the partition function (2.5)

$$Z = \sum_{\sigma_l=\pm 1} J \exp \left\{ - \sum_l (2\lambda c_1 + m_1) \sigma_l - \lambda \sum_t [c_2(\sigma_1 \sigma_2 + \sigma_1 \sigma_l + \sigma_2 \sigma_l) + c_3 \sigma_1 \sigma_2 \sigma_l] \right\}, \quad (2.12)$$

with  $J = \exp(-\lambda N_2 c_0 - N_1 m_0)$  and  $N_2$  denoting the total number of triangles. If we view  $\sigma_l$  as a spin variable and identify the corresponding link  $l$  of the triangulation with a lattice site, then  $Z$  reads as the partition function of a spin system with two- and three-spin nearest-neighbor interactions on a Kagomé lattice. A particularly simple form of Eq. (2.12) is obtained if one chooses  $m_1 = -2\lambda c_1$ , and therefore

$$m = -\frac{2\lambda c_1}{M}, \quad (2.13)$$

which is henceforth used for the measure in the  $Z_2$ RM as well as in SRC.

### III. OBSERVABLES AND SCALING RELATIONS

To compare both models we examined the quadratic link lengths and the area fluctuations on the simplicial lattice. Additionally we consider the squared curvature defined by

$$R^2 = \sum_i \frac{\delta_i^2}{A_i}. \quad (3.1)$$

Furthermore the Liouville mode is of special interest because it represents the only degree of freedom of pure 2d gravity. The discrete analogue  $\phi_i$  of the continuum Liouville field  $\varphi(x) = \ln \sqrt{g(x)}$  is defined by

$$\phi_i = \ln A_i, \quad A_i = \frac{1}{3} \sum_{t \supset i} A_t, \quad (3.2)$$

where  $A_i$  is the area element of site  $i$ . The Liouville susceptibility is then defined by

$$\chi_\phi = \langle A \rangle [\langle \phi^2 \rangle - \langle \phi \rangle^2], \quad (3.3)$$

where  $\phi = \frac{1}{A} \sum_i \phi_i$  and  $A$  is the total area [5]. From Ref. [5] it is known that for fixed total area  $A$  and the scale invariant measure  $dq/q$  the susceptibility scales according to

$$\ln \chi_\phi(L) \xrightarrow{L \rightarrow \infty} c + (2 - \eta_\phi) \ln L , \quad (3.4)$$

with  $L = \sqrt{A}$  and the Liouville field critical exponent  $\eta_\phi = 0$ .

One can easily derive a scaling relation for the SRC from the partition function (2.5) [12]. Rescaling all quadratic link lengths of Eq. (2.5) by a factor  $\zeta$ , i.e.  $q' = \zeta^{-1}q$ , yields

$$Z = \left[ \prod_l \int_0^\infty \zeta^{1-m} dq'_l q'^{-m} \right] \mathcal{F}_\eta(\{q'_l\}) e^{-\lambda \sum_i \zeta A'_i} . \quad (3.5)$$

Since this is only a change of the integration variables,  $Z$  cannot depend on  $\zeta$ . Hence we have

$$\frac{d \ln Z}{d \zeta} \Big|_{\zeta=1} = 0 = N_1(1-m) - \lambda \langle \sum_i A_i \rangle \quad (3.6)$$

and find that the expectation value of the area  $A$  is fixed to

$$\langle A \rangle = N_1 \frac{1-m}{\lambda} = N_1 \left( \frac{2c_1}{M} + \frac{1}{\lambda} \right) , \quad (3.7)$$

which is a useful identity to check the correctness of the simulation results.

For positive  $\lambda$  the scaling relation makes always sense, and we expect the partition function (2.5) to behave well. However, there is also a range for negative values of  $\lambda < \lambda_{c,scal} \equiv -M/2c_1$ , where the area expectation value remains positive. For our choice of  $\epsilon = 0.5$  one obtains  $M = 0.5493\dots$  and  $c_1 = 0.0788\dots$ , such that this value equates to  $\lambda_{c,scal} = -3.4817$ . For values of  $\lambda_{c,scal} < \lambda < 0$  the area expectation value is negative and hence the partition function (2.5) is ill-defined.

#### IV. SIMULATION DETAILS AND RESULTS

We studied the partition functions (2.5) and (2.12) on toroidal lattices with  $N_0 = 16 \times 16 = 256$  sites, resulting in  $N_1 = 768$  and  $N_2 = 512$ . The measure was chosen as a function of  $\lambda$  according to  $m = -\frac{2\lambda c_1}{M} = \lambda/\lambda_{c,scal}$  with  $\epsilon = 0.5$ , i.e.,  $m \approx -0.3\lambda$ . In the

SRC formulation we used a standard Metropolis algorithm to update every link during a lattice sweep. For each  $\lambda$  in the range of  $1 - 30$ , starting from an initial configuration with equilateral triangles, we first thermalized the system and then collected 200k measurements taken every 50<sup>th</sup> MC sweep. Error bars were computed by the standard Jackknife method on the basis of 10 blocks. The integrated autocorrelation time  $\tau_A$  for the area was in the range of unity, whereas the integrated autocorrelation time  $\tau_{R^2}$  of  $R^2$  was about 100 – 500, and  $\tau_\phi$  of  $\phi$  was about 100 – 1000, depending on the parameter  $\lambda$ .

For the update of the spins in the  $Z_2$ RM formulation we also used a Metropolis algorithm. Here we performed 100k MC update sweeps measuring every 10<sup>th</sup> sweep after an initial equilibration period. The integrated autocorrelation times were typically of the order one.

In our first test runs of SRC with positive  $\lambda$  we noticed that our measured area expectation value was not in agreement with the scaling relation (3.7), and that the mismatch was growing when we increased  $\lambda$ . A way to cure this problem was to implement a new global MC move, which we termed the *breathing move*. It simply consists of rescaling all quadratic link lengths  $q$  by a factor  $\zeta$ , which is the same as scaling the total area by the factor  $\zeta$ , where  $\zeta$  can be smaller or larger than one. Again, the usual Metropolis criterion was used to accept or reject this proposal, and the extent of  $\zeta$  was adjusted to yield an acceptance rate of roughly one half. We allowed for ten global breathing moves followed by a complete sweep through the lattice with normal link updates. Applying these two moves the area expectation value decreases with increasing  $\lambda$  in perfect agreement with the scaling relation (3.7), see the upper left plot in Fig. 1. For sake of better comparison observables are plotted in Fig. 1 and 2 relative to the critical cosmological constant,  $\lambda^* = \lambda - \lambda_c$  ( $= \lambda$  for SRC).

With the above global scaling one can also show that the area expectation value, which follows from the scaling relation for  $\lambda < \lambda_{c,scal}$ , is an unstable equilibrium value. This can be seen by considering the ratio of the Boltzmann factors  $B$  before and after a proposed global move, where we set  $q^{\text{new}} = \zeta q^{\text{old}}$  and  $A^{\text{new}} = \zeta A^{\text{old}}$ , with  $\zeta = 1 + \kappa$  and  $m = 1 - \alpha$ . Using these abbreviations we get

$$\begin{aligned}
\frac{B^{\text{new}}}{B^{\text{old}}} &= \frac{\exp(-\lambda\zeta A^{\text{old}} + \alpha \sum \ln \zeta q^{\text{old}})}{\exp(-\lambda A^{\text{old}} + \alpha \sum \ln q^{\text{old}})} \\
&= \exp(-\lambda\kappa A^{\text{old}} + \alpha \sum \ln(1 + \kappa)) \\
&\approx \exp(-\kappa\{\lambda A^{\text{old}} - \alpha N_1\} - \frac{\alpha N_1}{2}\kappa^2 + \dots).
\end{aligned} \tag{4.1}$$

The moves are always accepted in the Monte Carlo simulations if  $\frac{B^{\text{new}}}{B^{\text{old}}} > 1$ . The first term in the argument of the exponential is linear in  $\kappa$  and constitutes essentially the scaling relation (3.7). The second term quadratic in  $\kappa$  is *always positive* for negative  $\lambda < \lambda_{c,\text{scal}}$ , i.e., for negative  $\alpha$ . Therefore this term will initially drive the system away from its equilibrium value. In the next steps, the linear term amplifies the instability and, depending on the arbitrary initial sign of  $\kappa$ , the area will tend to zero or infinity.

However, even with the refined update scheme we observed that the SRC system thermalizes extremely slowly for very small  $\lambda$  and therefore display only statistically reliable data points for  $\lambda \geq 1$  in the plots on the l.h.s. of Figs. 1 and 2. One also expects that expectation values of the average squared link length  $q$  will decrease and that expectation values of the squared curvature will increase with growing  $\lambda$  which is indeed confirmed by the simulation results displayed in Fig. 1. The Liouville field  $\langle \phi \rangle$  and the associated susceptibility (3.3) are shown on the l.h.s. of Fig. 2. The peak in the Liouville susceptibility can be expected to move towards  $\lambda = 0$  for  $L \rightarrow \infty$  due to the diverging area at this point.

The corresponding quantities of the  $Z_2$ RM are shown for comparison on the r.h.s. of Figs. 1 and 2. Since it is a crude approximation a quantitative agreement with SRC cannot be expected. We see, however, that the two formulations yield for most quantities the same qualitative behavior for positive couplings  $\lambda^*$ . Whereas the SRC becomes ill-defined for negative  $\lambda^*$ , the  $Z_2$ RM as an effective spin system is well-defined for all values of the cosmological constant. In all quantities of the  $Z_2$ RM we observe the signature of a crossover or phase transition, which is particularly pronounced in the Liouville susceptibility. From the peak location we read off a critical coupling  $\lambda_c \approx -11$ . The phase transition in the  $Z_2$ RM might be viewed as some relic of the transition from a well- to an ill-defined regime of SRC. To get some idea on the nature of the phase transition we looked at the histograms

of the total area and the squared curvature in Fig. 3. They show a single-peak structure at  $\lambda_c$  which would hint at a continuous transition.

By performing several runs, we further have monitored the scaling of the Liouville susceptibility maxima in the  $Z_2$ RM for lattice sizes up to  $L = 256$ . The double-logarithmic plot in Fig. 4 shows that the scaling behavior (3.4) is governed by a critical exponent  $\eta_\phi \approx 2$ . We have performed a finite-size scaling analysis of the Liouville susceptibility on lattice sizes  $L = 4, 8, 12, 16, 24$ , and 32 also for SRC. Because of the transition to an ill-defined phase making computations in its vicinity difficult we employed in all simulations a fixed value  $\lambda = 1$  closest to the critical coupling (see Figs. 1 and 2). The Liouville-field exponent gives the behavior of the Liouville field in a specific phase, here the well-defined phase, and hence should be independent of  $\lambda$ . After an equilibration period we performed 20k - 100k measurements of the Liouville field and computed the associated susceptibility (3.3). Our results presented in Fig. 4 indeed show that we obtain the same value of  $\eta_\phi \approx 2$ , consistent with the results found in the  $Z_2$ RM. Furthermore, first results demonstrate scaling of physically relevant quantities with the number of allowed values for  $\sigma_l$  indicating universality between the  $Z_2$ RM, SRC and models “in between” [14].

Thus we observe strong disagreement with the Liouville value  $\eta_\phi = 0$ , which has been found for SRC with the scale invariant measure  $dq/q$  and fixed area constraint [5]. There the same lattice transcription as in the present study was employed and it seems reasonable to attribute the value  $\eta_\phi = 0$  to the scale invariance of the measure, whereas our measure  $dq/q^m$  with  $m$  given in (2.13) explicitly breaks scale invariance. One therefore might not be surprised to observe a different value of  $\eta_\phi$ .

## V. MEAN-FIELD CALCULATION FOR THE $Z_2$ -REGGE MODEL

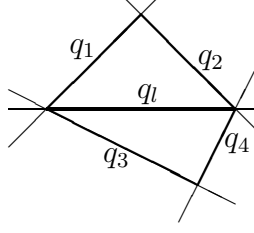
The variational derivation of mean-field theory [15] starts with a partition function

$$Z = \sum_{\{\sigma\}} \exp [-\beta H(\{\sigma\})] . \quad (5.1)$$

The comparison with equation (2.12) leads to

$$Z = \sum_{\{\sigma\}} J \exp \left( -\beta \left\{ - \sum_l \left[ \bar{Q}_1 + (\sigma_1 + \sigma_2 + \sigma_3 + \sigma_4) + \bar{Q}_3 (\sigma_1 \sigma_2 + \sigma_3 \sigma_4) \right] \sigma_l \right\} \right) , \quad (5.2)$$

with  $\beta = -\frac{1}{2}\lambda c_2$ ,  $\bar{Q}_1 = \frac{4c_1}{c_2} + \frac{2m_1}{\lambda c_2}$  and  $\bar{Q}_3 = \frac{2c_3}{3c_2}$ . The spins  $\sigma_j, j = 1, \dots, 4$ , correspond to the squared edge lengths  $q_j = 1 + \epsilon \sigma_j$  of the two triangles which have  $q_l$  and hence  $\sigma_l$  in common:



Now the Hamiltonian is divided into two parts,  $H = H_0 + H_1$ , where the choice of  $H_0$  is only governed by the requirement that it should be possible to evaluate the corresponding partition function  $Z_0$  analytically. With the mean-field Ansatz

$$H_0 = -\frac{M_0}{\beta} \sum_i \sigma_i \quad (5.3)$$

we get

$$Z_0 = \sum_{\{\sigma\}} \exp \left( M_0 \sum_i \sigma_i \right) = \left( e^{M_0} + e^{-M_0} \right)^{N_1} = 2^{N_1} \cosh^{N_1}(M_0) \quad (5.4)$$

for the partition function. According to Peierls's inequality we obtain for

$$Z = e^{-\beta F} = Z_0 \langle e^{-\beta(H-H_0)} \rangle_0 \geq Z_0 e^{-\beta \langle H - H_0 \rangle_0} = e^{-\beta F_{mf}} \quad (5.5)$$

a lower bound with the mean-field free energy

$$-\beta F_{mf} = \ln Z_0 - \beta \langle H - H_0 \rangle_0 . \quad (5.6)$$

The term  $\langle \dots \rangle_0$  represents the average with respect to the system described by  $H_0$ , i.e.

$$\begin{aligned} \langle H - H_0 \rangle_0 = & -\frac{1}{Z_0} \sum_{\{\sigma_i\}} \sum_l \left[ \bar{Q}_1 + (\sigma_1 + \sigma_2 + \sigma_3 + \sigma_4) + \bar{Q}_3 (\sigma_1 \sigma_2 + \sigma_3 \sigma_4) - \right. \\ & \left. - \frac{M_0}{\beta} \right] \sigma_l e^{M_0 \sum_i \sigma_i} . \end{aligned} \quad (5.7)$$

Because the thermal average or “mean” value of the spin results in

$$\langle \sigma \rangle_0 = \frac{e^{M_0} - e^{-M_0}}{e^{M_0} + e^{-M_0}} = \tanh(M_0) , \quad (5.8)$$

the different terms in (5.7) give

$$\begin{aligned} \langle \sum_l \sigma_l \rangle_0 &= N_1 \tanh(M_0) , \\ \langle \sum_l [(\sigma_1 + \sigma_2 + \sigma_3 + \sigma_4) \sigma_l] \rangle_0 &= 4N_1 (\tanh(M_0))^2 , \\ \langle \sum_l [(\sigma_1 \sigma_2 + \sigma_3 \sigma_4) \sigma_l] \rangle_0 &= 2N_1 (\tanh(M_0))^3 . \end{aligned} \quad (5.9)$$

Thus we get a  $\beta$ - and  $M_0$ -dependent expression for the mean-field free energy per link,

$$\begin{aligned} \beta f_{mf} \equiv \frac{\beta F_{mf}}{N_1} &= -\ln 2 - \ln (\cosh(M_0)) - 4\beta (\tanh(M_0))^2 - 2\bar{Q}_3 \beta (\tanh(M_0))^3 + \\ &+ (M_0 - \beta \bar{Q}_1) \tanh(M_0) , \end{aligned} \quad (5.10)$$

that has to be minimized ( $Z \geq \exp[-\beta F_{mf}]$ ). Differentiating (5.10) with respect to  $M_0$  leads to the mean-field equation

$$\tanh(M_0) + \frac{3\bar{Q}_3}{4} (\tanh(M_0))^2 = \frac{M_0}{8\beta} - \frac{\bar{Q}_1}{8} \quad (5.11)$$

for the free energy. We restrict ourselves again to a calculation without external field  $\bar{Q}_1$ . A trivial solution of (5.11) is  $M_0 = 0$  yielding  $\beta f_{mf} = -\ln 2$ , which is the stable solution for small  $\beta$  (high “temperature”). With increasing  $\beta$  a second minimum develops whose free energy is eventually lower than that of the  $M_0 = 0$  solution. This corresponds to the first-order phase transition expected due to the cubic term in (5.10). To locate the transition point we proceed as follows. For a given  $M_0$  value ( $< 0$ ) we can read off  $\beta$  directly from Eq. (5.11), without solving any non-linear equation. By inserting  $M_0$  and  $\beta$  in (5.10) we obtain immediately the free energy which can then be plotted versus  $\beta$  as in Fig. 5. This curve is double valued because a given  $M_0$  value can correspond to the minimum (lower branch) or the maximum (upper branch) of  $\beta f_{mf}$  at a fixed  $\beta$ . It should be remarked that for  $\beta > 0.125$  there is another meta-stable solution with  $M_0 > 0$  which is not displayed here. With decreasing  $\beta$  the free energy of the non-trivial solution increases until at  $\beta_{c,mf}$  it hits the

value of the  $M_0 = 0$  solution. For  $\beta < \beta_{c,mf}$  the non-trivial solution first becomes meta-stable and then disappears completely (at the point where the minimum- and maximum-branch merge). In this way it is straightforward to extract the transition point as

$$\beta_{c,mf} \approx 0.1174 \text{ corresponding to } \lambda_{c,mf} \approx -8.0 \text{ with } \epsilon = 0.5 . \quad (5.12)$$

At this value the free energy shows a structure with two minima of identical height (cf. Fig. 6), which reconfirms that the mean-field calculation for the  $Z_2$ -Regge Model predicts a (weak) first-order phase transition. The value (5.12) is slightly below the numerical estimate of  $\lambda_c \approx -11$ ; however, it is a well-known property of mean-field theory to underestimate the critical coupling. In fact, the ratio between the mean-field and the numerical value,  $\frac{\lambda_{c,mf}}{\lambda_c} \approx 0.73$ , is of the same order of magnitude as the corresponding quantity for the exactly solvable two dimensional Ising model on a square lattice where  $(\frac{\lambda_{c,mf}}{\lambda_{c,exact}})_I \approx 0.567$ .

## VI. CONCLUSIONS

The aim of this work was to examine whether the  $Z_2$ RM allowing for two discrete edge lengths is an appropriate simplification of the SRC with continuously varying edge lengths in two dimensions. We studied both models by means of Monte Carlo simulations and found that the simpler  $Z_2$ RM qualitatively reproduces the behavior of physical observables like the Liouville field or the squared curvature for the bare coupling  $\lambda > 0$ . A finite-size scaling analysis of the Liouville susceptibility yields for both models the same critical exponent  $\eta_\phi \approx 2$ . This hints at a continuous phase transition which is also necessary to perform a continuum limit. Concerning universality it is a non-trivial result, because in the SRC model with scale invariant measure a value of  $\eta_\phi = 0$  was found.

To obtain further insight, mean-field theory was applied to the  $Z_2$ RM indicating a weak first-order phase transition. This would prevent one to gain important information about the continuum theory. However, the numerical simulations indicate that fluctuations, which are neglected in mean-field theory, soften the true nature of the phase transition to second order. The details of this transition such as critical exponents etc. are still left to be determined.

An interesting question is the influence of allowing for more than two link lengths and the convergence of the properties of such an extended  $Z_2$ RM to those of SRC in two dimensions [14]. With additional degrees of freedom the situation might resemble the more involved four-dimensional case where one has to deal with 10 edges per simplex and the non-trivial Einstein-Hilbert action  $\sum_{t \supset i} \delta_t A_t$  with 50 triangles  $t$  per vertex  $i$  in Eq. (2.1). Thus the action  $I(q)$  takes on a large variety of values already for  $Z_2$ RM and therefore SRC can be approximated more accurately [16].

## ACKNOWLEDGMENTS

A. H. acknowledges support from an Erasmus grant during his stay at the FU Berlin, where this project was started. J. R. was supported by Fonds zur Förderung der wissenschaftlichen Forschung under contract P11141-PHY. W. J. thanks the Deutsche Forschungsgemeinschaft for a Heisenberg Fellowship, and also acknowledges partial support by the German-Israel-Foundation (GIF) under contract No. I-0438-145.07/95. Parts of the numerical simulations were performed on the North German Vector Cluster (NVV) under grant bvpf01.

## REFERENCES

- [1] T. Regge, *Nuovo Cimento* **19**, 558 (1961).
- [2] N.H. Christ, R. Friedberg, and T.D. Lee, *Nucl. Phys.* **B202**, 89 (1982); J. Cheeger, W. Müller, and R. Schrader, *Comm. Math. Phys.* **92**, 405 (1984); H.W. Hamber, *Nucl. Phys.* **B** (Proc. Suppl.) **99A**, 1 (1991); J. Ambjørn, in *Proceedings of the 1994 Les Houches Summer School, Session LXII*; J. Ambjørn, *Nucl. Phys.* **B** (Proc. Suppl.) **42**, 3 (1995); S. Catterall, *Nucl. Phys.* **B** (Proc. Suppl.) **47**, 59 (1996); D.A. Johnston, *Nucl. Phys.* **B** (Proc. Suppl.) **53**, 43 (1997).
- [3] V. Kazakov, *JETP Lett.* **44**, 133 (1986); *Phys. Lett.* **A119**, 140 (1986).
- [4] H. Hamber, *Nucl. Phys.* **B400**, 347 (1993); H. Hamber and R. Williams, *Nucl. Phys.* **B435**, 361 (1995); W. Beirl, E. Gerstenmayer, H. Markum, and J. Riedler, *Phys. Rev.* **D49**, 5231 (1994); W. Beirl, H. Markum, and J. Riedler, *Phys. Lett.* **B341**, 12 (1994); B. Berg and B. Krishnan, *Phys. Lett.* **B318**, 59 (1993); W. Beirl, B. Berg, B. Krishnan, H. Markum, and J. Riedler, *Phys. Lett.* **B348**, 355 (1995); C. Holm and W. Janke, *Nucl. Phys.* **B477**, 465 (1996); *Phys. Lett.* **B375**, 9 (1996); *Phys. Lett.* **B390**, 59 (1997).
- [5] M. Gross and H. Hamber, *Nucl. Phys.* **B364**, 703 (1991); C. Holm and W. Janke, *Phys. Lett.* **B335**, 143 (1994).
- [6] T. Fleming, M. Gross, and R. Renken, *Phys. Rev.* **D50**, 7363 (1994); W. Beirl, H. Markum, and J. Riedler, *Int. J. Mod. Phys.* **C5**, 359 (1994); W. Beirl, P. Homolka, B. Krishnan, H. Markum, and J. Riedler, *Nucl. Phys.* **B** (Proc. Suppl.) **42**, 710 (1995).
- [7] V. Kazakov, *Phys. Lett.* **B150**, 282 (1985); F. David, *Nucl. Phys.* **B257**, 45 (1985); J. Ambjørn, B. Durhuus, and J. Fröhlich, *Nucl. Phys.* **B257**, 433 (1985); V. Kazakov, I. Kostov, and A. Migdal, *Phys. Lett.* **B157**, 295 (1985).
- [8] V. Knizhnik, A. Polyakov, and A. Zamolodchikov, *Mod. Phys. Lett.* **A3**, 819 (1988).

[9] J. Ambjørn, J. Nielsen, J. Rolf, and G. Savvidy, *Class. Quant. Grav.* **14**, 3225 (1997);  
H. Hamber and R. Williams, hep-th/9708019.

[10] P. Menotti, *Nucl. Phys. B* (Proc. Suppl.) **63**, 760 (1998); P. Menotti and P. Peirano, *Phys. Lett. B* **353**, 444 (1995); *Nucl. Phys. B* **473**, 426 (1996); *Nucl. Phys. B* (Proc. Suppl.) **53**, 780 (1997); *Nucl. Phys. B* (Proc. Suppl.) **57**, 82 (1997); *Nucl. Phys. B* **488**, 719 (1997).

[11] J.B. Hartle, *J. Math. Phys.* **26**, 804 (1985); *J. Math. Phys.* **27**, 287 (1986).

[12] H. Hamber and R. Williams, *Nucl. Phys. B* **248**, 392 (1984); *Nucl. Phys. B* **269**, 712 (1986).

[13] A. Jevicki and M. Ninomiya, *Phys. Lett.* **150B**, 115 (1985); M. Roček and R. Williams, *Phys. Lett. B* **104**, 31 (1981); *Z. Phys. C* **21**, 371 (1984).

[14] E. Bittner, H. Markum, and J. Riedler, *Nucl. Phys. B* (Proc. Suppl.), in print; hep-lat/9809135.

[15] J. Binney, N. Dowrick, A. Fisher, and M. Newman, *The Theory of Critical Phenomena* (Oxford University Press, Oxford, 1992).

[16] W. Beirl, A. Hauke, P. Homolka, B. Krishnan, H. Kröger, H. Markum, and J. Riedler, *Nucl. Phys. B* (Proc. Suppl.) **47**, 625 (1996); P. Homolka, W. Beirl, P. Homolka, H. Markum, J. Riedler, and H. Kröger, *Nucl. Phys. B* (Proc. Suppl.) **53**, 769 (1997).

## FIGURES

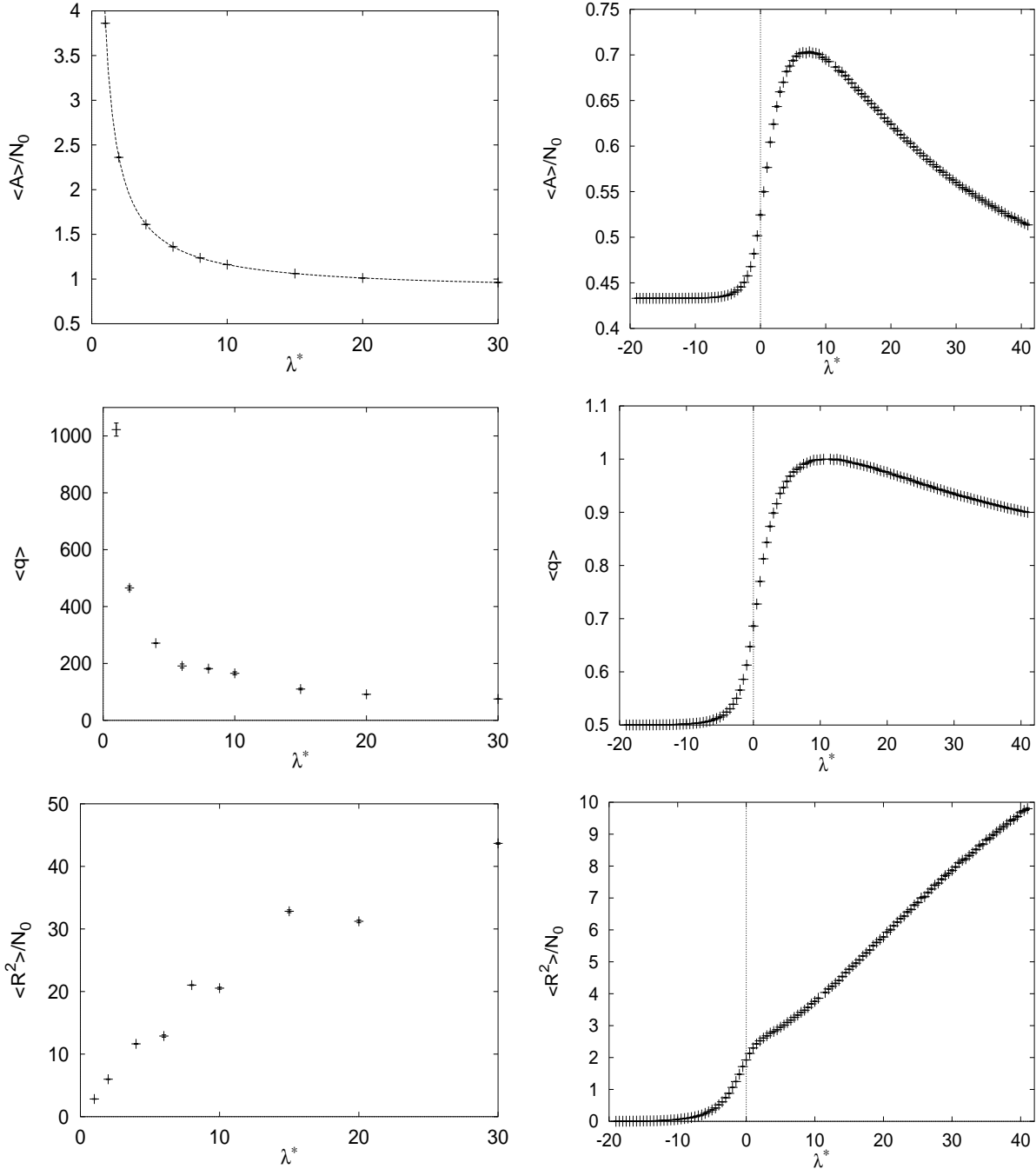


FIG. 1. Expectation values of the area  $A$ , the average squared link length  $q$ , and the squared curvature  $R^2$  as a function of the distance to the critical cosmological constant  $\lambda^*$  for the Standard Regge Calculus (left plots) and the  $Z_2$ -Regge Model (right plots).  $N_0$  is the total number of vertices.

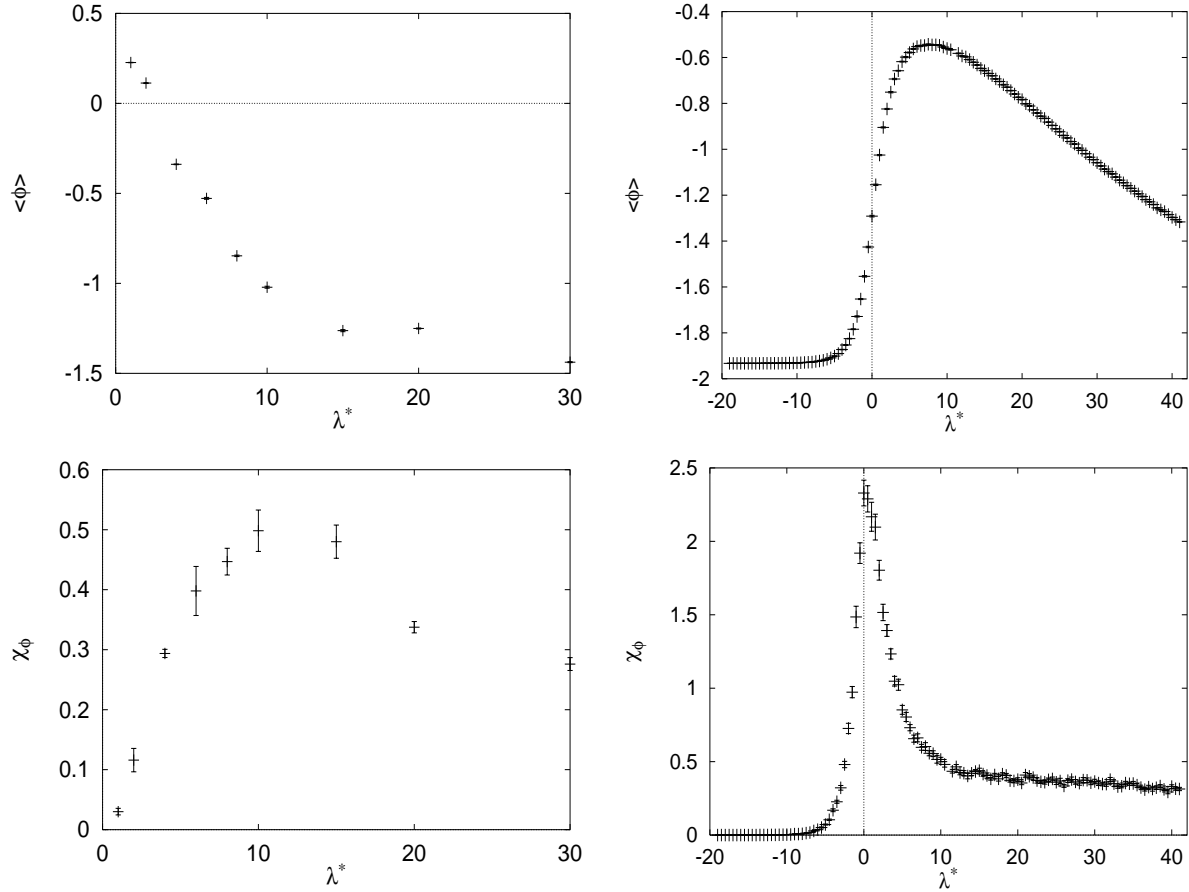


FIG. 2. Expectation values of the Liouville field  $\phi$  and the Liouville field susceptibility  $\chi_\phi$  as a function of  $\lambda^*$  for the Standard Regge Calculus (left plots) and the  $Z_2$ -Regge Model (right plots).

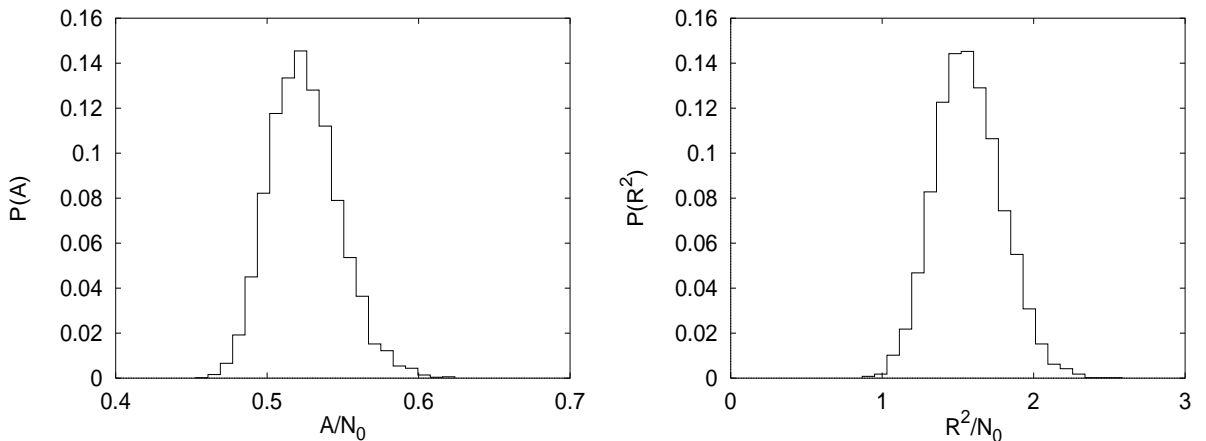


FIG. 3. Histograms of the total area and the squared curvature per vertex at the transition point of the  $Z_2$ -Regge Model.

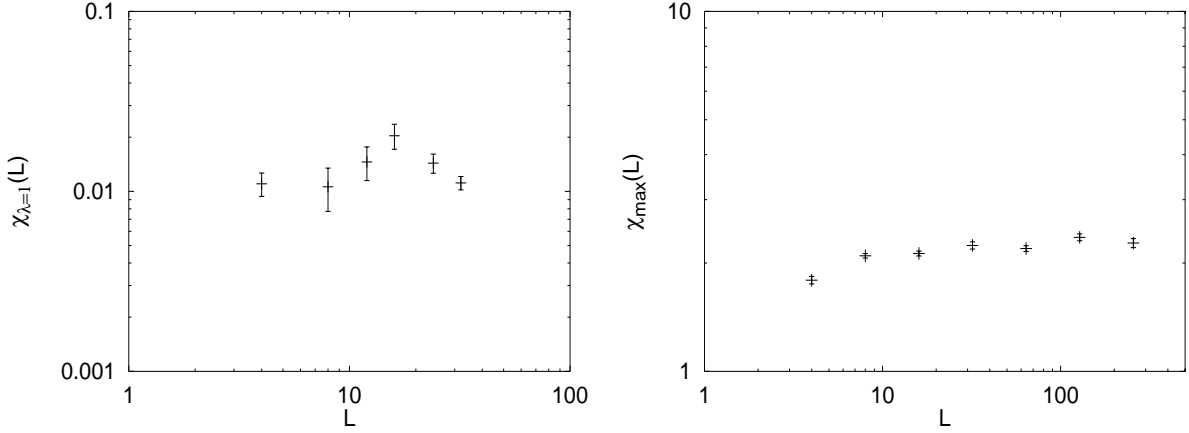


FIG. 4. Scaling of the of the Liouville field susceptibility  $\chi_\phi$  as a function of the lattice size  $L$  for the SRC (left) at  $\lambda = 1$  and the  $Z_2$ RM (right) for  $\max(\chi_\phi)$ .

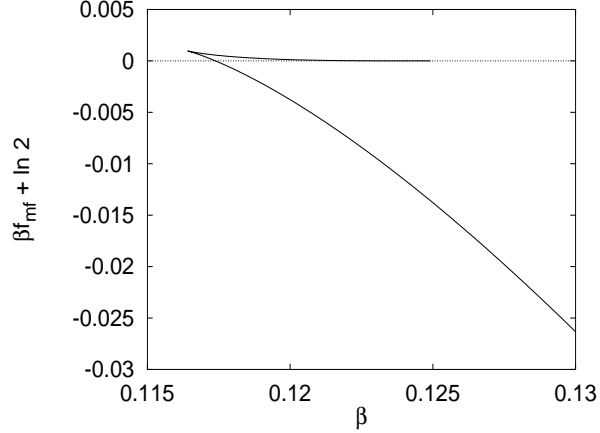


FIG. 5. Value of  $\beta f_{mf} + \ln 2$  at the two minima under variation of  $\beta$ .

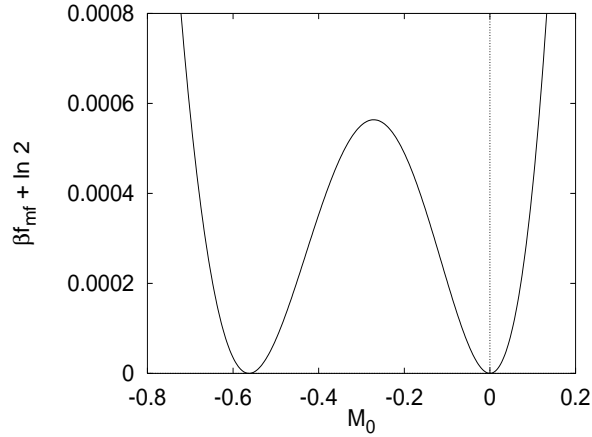


FIG. 6. Free energy  $\beta f_{mf} + \ln 2$  as a function of  $M_0$  at the mean-field transition point.